Numerical Analysis of Carrier-Depletion Strained SiGe Optical Modulators With Vertical p-n Junction

Younghyun Kim, Mitsuru Takenaka, *Member, IEEE*, and Shinichi Takagi, *Member, IEEE*

***Abstract*— The modulation characteristics of carrier-depletion strained SiGe optical modulators with a vertical p-n junction are numerically analyzed by technology computer-aided design simulation and finite-difference optical mode analysis. In addition to the strong optical confinement in the vertical direction for the fundamental transverse electric field mode, the vertical p-n junction effectively depletes the strained SiGe layer in which the plasma dispersion effect is enhanced owing to the mass modulation of holes by strain. We predict that a $Si_{0.7}Ge_{0.3}$ optical modulator exhibits $V_\pi L$ at 1.55 μm of as small as 0.31 V-cm at a bias voltage of −2 V, which is ∼1.8 times smaller than that of a Si optical modulator. The product of $V_\pi L$ and the phase-shifter loss ($\alpha V_\pi L$) is also expected to be as low as 18.3 V-dB at −2 V, enabling optical modulation with a 5-dB extinction ratio in a symmetric Mach–Zehnder modulator.**

***Index Terms*— Strained SiGe, optical modulator, vertical *p-n* junction, Si photonics.**

I. Introduction

SILICON-BASED optical modulators have been intensely developed in the past ten years as one of the important building blocks for optical interconnects [1]. Many types of Si-based optical modulators based on free-carrier effects [2]–[6] and electric-field effects [7]–[9] have been demonstrated so far. Among them, depletion-type Si optical Mach-Zehnder interferometer (MZI) modulators with a *p-n* junction based on the plasma dispersion effect have been mostly reported because of the high modulation speed over a broad wavelength range. High-speed modulation of up to 50 Gbps has been demonstrated by taking advantage of the fast response of majority carriers in carrier depletion [10], [11]. However, the modulation efficiency $V_\pi L$ of Si optical modulators with a lateral *p-n* junction is typically 1 to 4 V-cm because of the weak plasma dispersion effect in Si, where $V_\pi L$ is defined as the product of the driving voltage and the phase-shifter length required for a π phase shift. As a result, a long phase-shifter length or a high driving voltage is necessary for MZI modulators [12], [13]. Although it is possible to reduce $V_\pi L$ for carrier-depletion-type Si MZI modulators by increasing the doping concentration of the *p-n* junction in the waveguide core, an increase in the insertion loss of the phase shifter is unavoidable because of the increase in the free-carrier absorption. To take into account the phase-shifter loss, the product of $V_\pi L$ and the phase-shifter loss ($\alpha V_\pi L$) has been recently suggested as a new figure of merit [14]. $\alpha V_\pi L$ is generally higher in the case of highly doped modulators designed to have a low $V_\pi L$. Therefore, it is important to reduce $\alpha V_\pi L$ in addition to reducing $V_\pi L$ [15]. For this purpose, we have proposed compressively strained SiGe-based optical modulators, in which the enhancement of the plasma dispersion effect is expected by reducing the effective mass of holes in strained SiGe [16]. Recently, we have experimentally demonstrated the enhanced plasma dispersion effect and free-carrier absorption in a carrier-injection strained SiGe modulator [17]. Owing to the enhanced plasma dispersion effect, the reduction of $\alpha V_\pi L$ is expected in a carrier-depletion strained SiGe modulator as compared with that in a Si modulator.

In this paper, we numerically analyze the modulation characteristics at 1.55 μm of carrier-depletion strained SiGe optical modulators with a vertical *p-n* junction by technology computer-aided design (TCAD) simulation and finite-difference optical mode analysis. Since the optical confinement in the vertical direction is stronger than that in the lateral direction in a conventional rib waveguide on a silicon-on-insulator (SOI) substrate, the vertical *p-n* junction modulator exhibits better modulation efficiency than a lateral *p-n* junction modulator. The vertical *p-n* junction can also effectively deplete the strained SiGe layer, making it suitable for obtaining high modulation efficiency. It is predicted that a $Si_{0.7}Ge_{0.3}$ optical modulator exhibits $V_\pi L$ of as small as 0.31 V-cm at −2 V bias voltage, which is approximately 1.8 times smaller than that of Si optical modulator. Simultaneously, $\alpha V_\pi L$ can be maintained as low as 18.3 V-dB owing to the enhanced plasma dispersion effect in the strained SiGe layer.

II. Comparison of Lateral And Vertical p-n Junctions for Carrier-Depletion Modulators

We first compare the modulation efficiencies of carrier-depletion optical modulators between lateral and vertical

Manuscript received December 18, 2014; revised February 10, 2015; accepted February 18, 2015. Date of current version March 4, 2015. This work was supported by the New Energy and Industrial Technology Development Organisation within the Strategic Information and Communications Research and Development Promotion Programme through the Ministry of Internal Affairs and Communications Project entitled Integrated Photonics-Electronics Convergence System Technology.

The authors are with the Department of Electrical Engineering and Information Systems, The University of Tokyo, Tokyo 113-8654, Japan (e-mail: yhkim@mosfet.t.utokyo.ac.jp; takenaka@mosfet.t.u-tokyo.ac.jp; takagi@ee.t.utokyo.ac.jp).

Color versions of one or more of the figures in this paper are available online at http://ieeexplore.ieee.org.

Digital Object Identifier 10.1109/JQE.2015.2405931

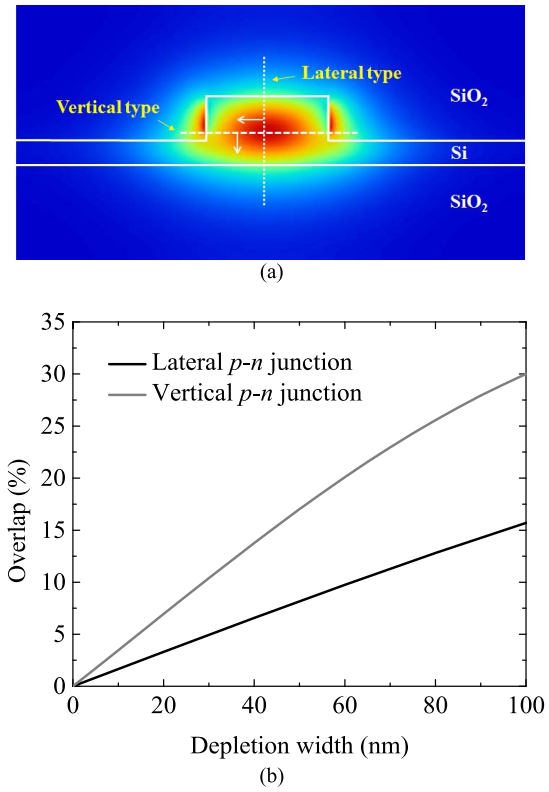

Fig. 1. (a) Fundamental TE mode of a rib waveguide on an SOI substrate, and (b) Overlap between depletion layer and TE mode in lateral and vertical depletion optical modulators as a function of depletion width.

p-n junctions by calculating the overlap between a depletion layer and the fundamental transverse electric field (TE) mode of a rib waveguide on an SOI substrate as shown in FPS Fig. 1(a). The fundamental TE field mode is calculated by finite-difference optical mode analysis using a rib waveguide with a 500-nm-wide and 170-nm-high mesa, assumed to be fabricated on a 220-nm-thick SOI wafer. The depletion layer is assumed to be depleted vertically or laterally from the center of the waveguide where the optical intensity is the greatest. The vertical depletion modulator has an approximately two times larger overlap between the depletion layer and the optical field than the lateral depletion modulator owing to the difference between the width and height of the waveguide core as shown in FPS Fig. 1(b). Since the modulation efficiency increases as the overlap increases, the carrier-depletion optical modulator with a vertical p-n junction is expected to show greater modulation efficiency than a modulator with a lateral p-n junction.

III. Design and Numerical Analysis

In Section II, we showed that a vertical p-n junction is approximately two times more effective than a lateral p-n junction. To utilize strained SiGe in conjunction with a vertical p-n junction, we propose a strained SiGe optical modulator with a vertical p-n junction as shown in Fig. 2. In this section, the modulation characteristics of the vertical p-n junction SiGe optical modulator will be discussed.

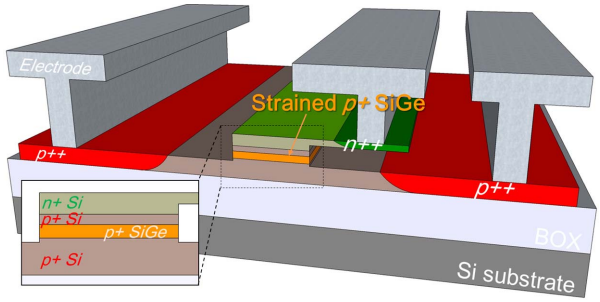

Fig. 2. Schematic of carrier-depletion type strained SiGe optical modulator with vertical p-n junction.

A. Device Structure

Figure 2 shows a schematic of the strained SiGe optical modulator with a vertical p-n junction. It consists of a 220-nm-thick and a 600-nm-wide waveguide rib. The slab thickness is assumed to be 50 nm in this study.

In the waveguide core, a 40-nm-thick strained $Si_{1-x}Ge_x$ layer is embedded, which can be coherently grown on Si (001) without defect-related losses when the Ge fraction is less than 0.3 [18]–[20]. Even though the bandgap shrinkage by strain induces optical loss when a photon energy at an operating wavelength is close to the narrowed bandgap energy, the optical loss of SiGe with approximately 30 % Ge fraction is negligible for an optical modulator application [21].

In the mesa, the thickness of the top n^+ Si layer is 60 nm and the total thickness of the p^+ Si/SiGe/Si layers is 160 nm including the 40-nm-thick SiGe. The thicknesses of p^+ Si layer will be discussed when describing the SiGe modulator.

The process of the proposed vertical type SiGe modulator is more complex than the lateral type modulator. However, strained SiGe itself has been already used in commercially available CMOS circuits. Thus, through CMOS-compatible process, the vertical layer structure in the phase shifter can be formed by buried regrowth with in-situ doping as like Ge photodetectors reported in [22]. Although carrier-accumulation modulators exhibit higher modulation efficiency, a lager capacitance in accumulation devices results in higher power consumption and lower speed operation than carrier-depletion devices. Therefore, the carrier-depletion type SiGe modulator with vertical p-n junction is more promising that a carrier-accumulation modulator in terms of simple process, low power and high speed.

To simulate the optical characteristics of modulators, Synopsys TCAD Sentaurus to calculate the carrier concentration in conjunction with a finite-difference mode solver for optical waveguides was used. The carrier concentration was calculated as a function of the applied DC reverse-bias between the p^{++} and n^{++} contact regions. We assume ohmic contact to the p^{++} and n^{++} regions with a doping concentration of 10^{20} cm^{-3} for boron and phosphorus, respectively. The electron density at the top of the n^+ region is assumed to be 5×10^{18} cm^{-3}, which is designed to decrease toward the boundary of the p-n junction as shown in Fig. 3 [23]. The electron density in the n^+ region at the p-n boundary is

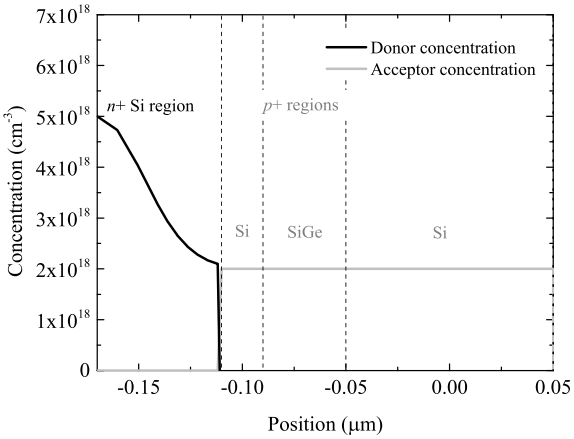

Fig. 3. Doping profile of [001]-direction at the center of waveguide for 2.0×10^{18} cm^{-3} of hole density case.

assumed to be the same as the hole density in the p^+ region. We assume that each p^+ region is uniformly doped. The electron density in the n^+ region is higher than the hole density in the p^+ region so that the depletion region mostly extends toward the p^+ region which includes the p^+ Si/SiGe/Si layers.

To evaluate the optical characteristics, the changes in the refractive index and absorption coefficient of SiGe and Si are calculated using Soref's equations [24] by taking into account the enhanced free-carrier effects in strained SiGe [16], [17]. The changes in the effective refractive index and absorption coefficient in the modulators are extracted by calculating the overlap between the carrier distributions and the optical field.

B. Optimization of Carrier-Depletion Si Optical Modulator With Vertical p-n Junction

First, we optimize the hole density of the p^+ region in the Si modulator with the vertical *p-n* junction, which has the greatest effect on the device performances. Here, we assume that the Ge fraction of the SiGe layer is 0 and all the p^+ regions are composed of p^+ Si with the same doping concentration. To optimize the hole density of the p^+ region, the modulation characteristics were investigated for hole densities ranging from 1.5×10^{17} to 3×10^{18} cm^{-3} in the p^+ region, which is less than the electron density in the n^+ region. Figure 4 shows the calculated change in the effective refractive index for various hole densities in the p^+ region as a function of reverse bias voltage. As the hole density increases, the effective refractive index increases due to the large change in the carrier density caused by depletion. When the hole density is 1.5×10^{17} cm^{-3}, saturation of the change in the effective refractive index is observed at -4 V because the depletion region reaches the bottom of the Si slab.

Figure 5 shows $V_\pi L$ as a function of reverse bias voltage. $V_\pi L$ also decreases with increasing hole density. When the hole density is larger than 1×10^{18} cm^{-3}, $V_\pi L$ of less than 1.0 V-cm is achievable with a reverse bias voltage of larger than -3 V. On the other hand, the phase-shifter loss at 0 V also increases with increasing hole density owing to

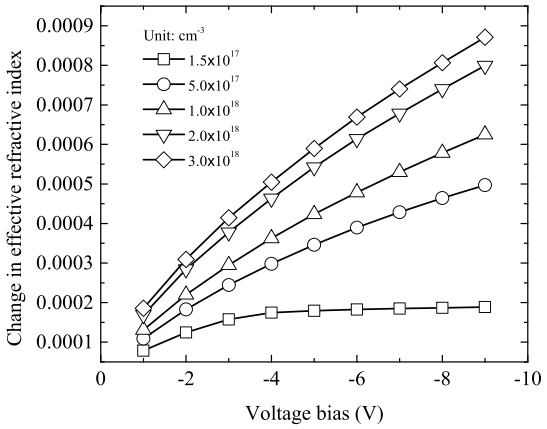

Fig. 4. Calculated change in effective refractive index with varied hole densities in the p^+ region as a function of reverse bias voltage.

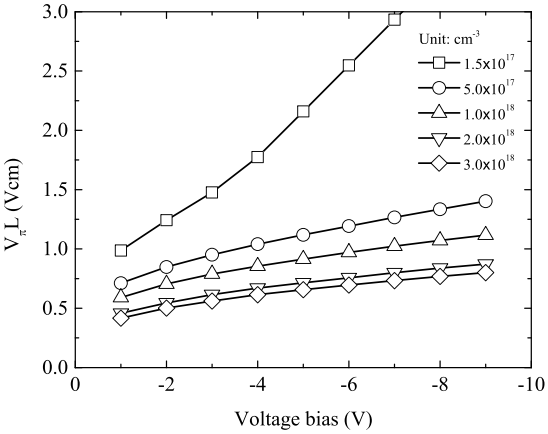

Fig. 5. $V_\pi L$ of the Si modulator as a function of reversed bias voltage.

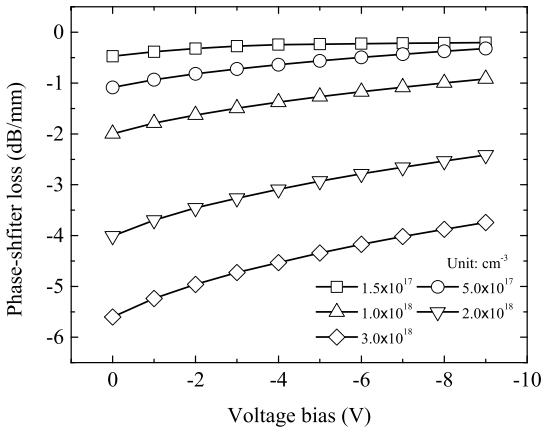

Fig. 6. Phase-shifter loss of the Si modulator at 0 V with varied hole density as a function of reverse bias voltage.

free-carrier absorption as shown in Fig. 6. The phase-shifter loss at 0 V is as large as -5.6 dB/mm at a hole density of 3×10^{18} cm^{-3}. The trade-off between the modulation efficiency and the phase-shifter loss in terms of the doping concentration is an important issue to be carefully considered. Also, the change in the phase-shifter loss becomes large with increasing hole density. For MZI modulators, a change in the phase-shifter loss affects the extinction ratio of modulation.

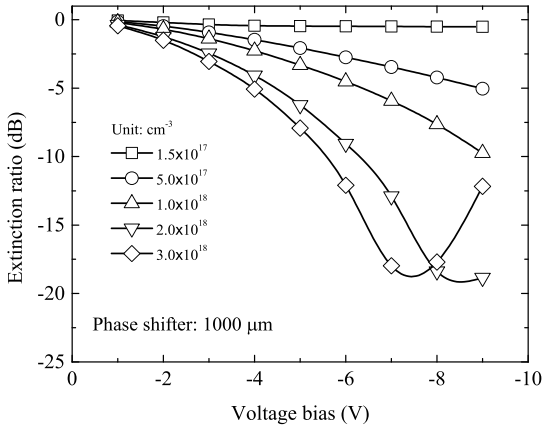

Fig. 7. Extinction ratio of symmetric Si MZI modulator as a function of reversed bias voltage.

Therefore, we also analyzed the extinction ratio of a symmetric MZI modulator, as shown in Fig. 7, which was calculated by the transfer-matrix method [25] with the assumption of the same phase-shifter loss at 0 V in both arms owing to the same doping density. The length of the phase shifter is assumed to be 1000 μm. A difference between the loss in the two arms is induced when a reverse bias voltage is applied to one arm. However, an extinction ratio of larger than 5 dB is still expected even when the hole density is as high as 2×10^{18} cm^{-3} at -5 V. As discussed here, we can achieve high modulation efficiency by using a doping concentration of $2 - 3 \times 10^{18}$ cm^{-3}. However, the insertion loss increases simultaneously as shown in Fig. 6. Hence, the enhancement of the plasma dispersion effect itself is essential to achieve high modulation efficiency and low insertion loss simultaneously.

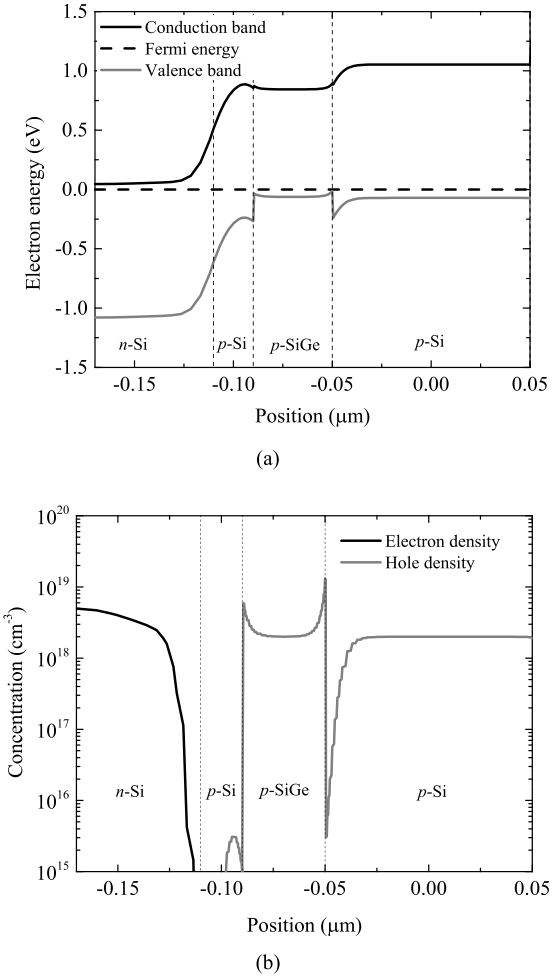

Fig. 8. (a) Band structure and (b) carrier distribution in [001] direction at the center of the waveguide with a hole doping density of 2.0×10^{18} cm^{-3}.

C. Carrier-Depletion SiGe Optical Modulator With Vertical p-n Junction

By considering the optimized structure of the Si optical modulator, we attempt to optimize the design of the carrier-depletion SiGe optical modulator with the vertical *p-n* junction. For the SiGe optical modulator, it is expected that the loss in the modulator will increase further as a result of the enhanced free-carrier absorption. Therefore, in the following analyses, a hole density of 2×10^{18} cm^{-3} is adopted to achieve a $\alpha V_\pi L$ value of approximately 18 V-dB, which is comparable to that for a low-doped Si modulator [14] as discussed later.

The proposed SiGe optical modulator has the Si/SiGe heterostructures in the waveguide core. The bandgap of strained SiGe is smaller than that of Si, resulting in the large band offset in the valence band. Therefore, the band alignment should be carefully considered since it affects carrier distribution and modulation efficiency. Figure 8 shows band structure and carrier distribution in [001] direction at the center of waveguide. The *p-n* junction is formed between *n*-Si and *p*-Si, showing the large band bending and the low carrier concentrations due to depletion as shown in Fig. 8 (a) and (b), respectively. It is worthy to note that holes are confined in the edges of SiGe because of the band offset in the valence band between SiGe and Si. It indicates that the modulation efficiency is expected to be further enhanced by confining more holes in the strained SiGe layer where the plasma dispersion is greater than Si layers.

First we optimize the thickness of the p^+ Si layer between the n^+ Si and p^+ SiGe layers. Even with no bias voltage, there is an initial depletion region at the junction. Thus, an appropriate thickness of the p^+ Si layer above the p^+ SiGe layer is important to ensure that depletion starts from the p^+ SiGe layer when a reverse bias voltage is applied. Figure 9 shows the change in the effective refractive index of the $Si_{0.7}Ge_{0.3}$ optical modulator for various p^+ Si thicknesses as a function of reverse bias voltage. When the reverse bias voltage increases, the change in the effective refractive index increases due to the extension of the depletion layer. As shown in Fig. 9, the largest change in the effective refractive index is obtained when the thickness of the p^+ Si layer ranges from 10 to 20 nm. There is no significant difference in the changes in the effective refractive index between 10-nm-thick and 20-nm-thick p^+ Si structures when the bias voltage is below -5 V. However, the change in the effective refractive index slightly degrades below a bias voltage of -6 V in the 10-nm-thick p^+ Si device because of the full depletion of the SiGe layer.

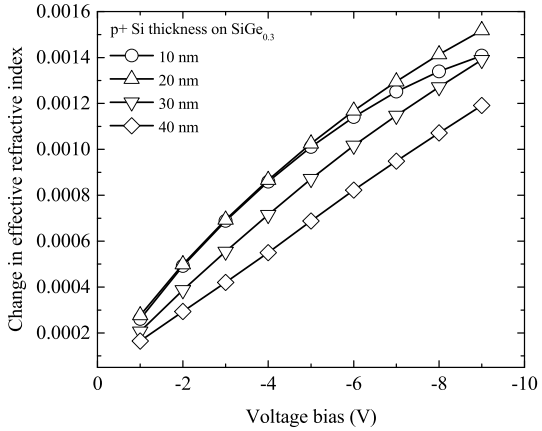

Fig. 9. Calculated change in effective refractive index strained SiGe optical modulator with varied p^+ Si thickness as a function of reversed bias voltage.

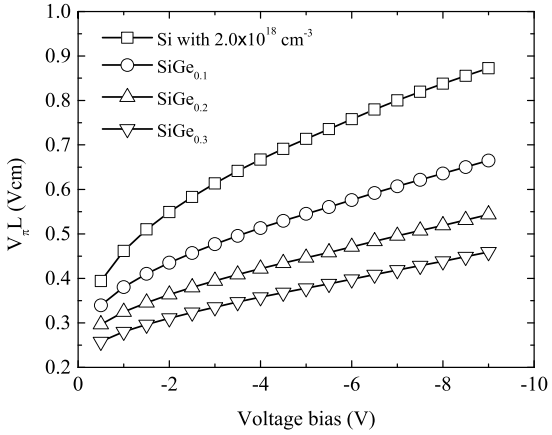

Fig. 11. $V_\pi L$ of strained SiGe optical modulator with different Ge fractions in SiGe alloy as a function of reversed bias voltage.

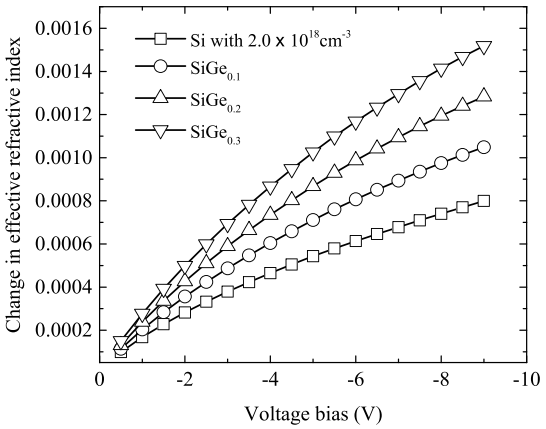

Fig. 10. Calculated change in effective refractive index of strained SiGe optical modulator with varied Ge fraction in SiGe alloy as a function of reversed bias voltage.

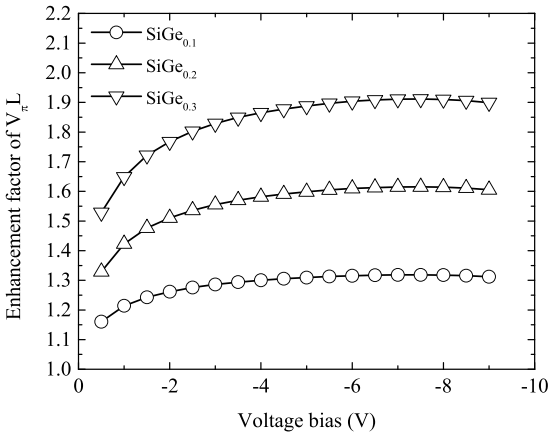

Fig. 12. Enhancement factor for $V_\pi L$ of strained SiGe optical modulator with varied Ge fractions in SiGe alloy as a function of reversed bias voltage.

Therefore, a 20-nm-thick p^+ Si layer is chosen for the SiGe optical modulator.

Figure 10 shows the dependence of the effective refractive index on the Ge fraction of the SiGe optical modulator. As the Ge fraction increases, the change in the effective refractive index increases thanks to the enhancement of the plasma dispersion effect in strained SiGe.

Figure 11 shows $V_\pi L$ for the SiGe optical modulator with various Ge fractions as a function of reverse bias voltage. $V_\pi L$ decreases with increasing Ge fraction due to the enhanced plasma dispersion effect. $V_\pi L$ is as low as 0.31 V-cm at -2 V when the Ge fraction is 0.3, which is approximately 1.8 times smaller than that of the Si modulator, as shown in Fig. 12.

In addition to the enhancement of the modulation efficiency, the insertion loss per unit length simultaneously increases with increasing Ge fraction as a result of the enhanced free-carrier absorption. Figure 13 shows the Ge fraction dependence of the insertion loss of the 1-mm-long phase shifter. The insertion loss of the phase shifter increases by approximately 2 dB/mm as the Ge fraction increases from 0 to 0.3, which is not significant because the modulation efficiency also increases, enabling a shorter phase shifter. To clarify the improvement

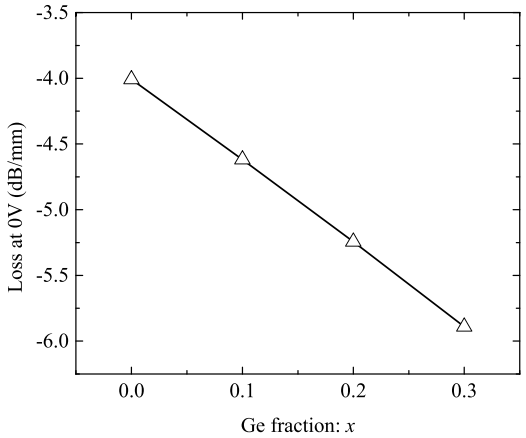

Fig. 13. Phase shifter loss at 0 V of strained SiGe optical modulator as a function of Ge fraction in SiGe alloy.

of the carrier-depletion optical modulator for strained SiGe, we show the enhancement factor for the change in effective refractive index divided by insertion loss at 0 V for each Ge fractions of SiGe in Fig. 14, taking into account the both enhanced plasma dispersion effect and free-carrier absorption

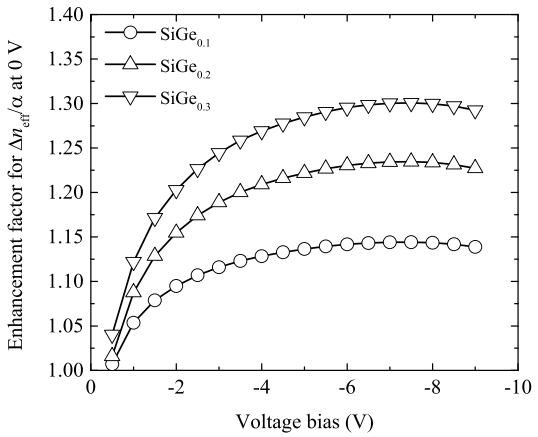

Fig. 14. Enhancement factor for change in effective refractive index divided by insertion loss at 0 V.

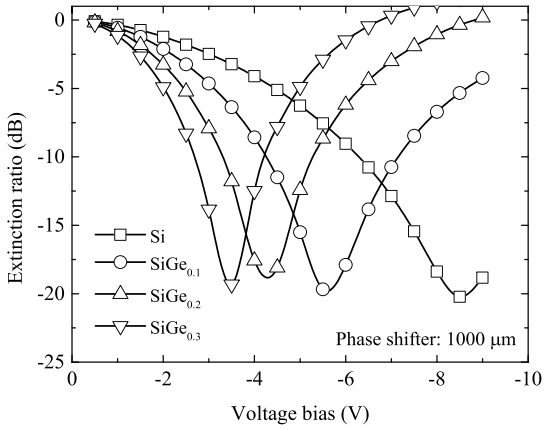

Fig. 15. Extinction ratio of vertical *p-n* junction carrier-depletion type strained SiGe optical modulator with different Ge fractions in SiGe alloy as a function of reversed bias voltage.

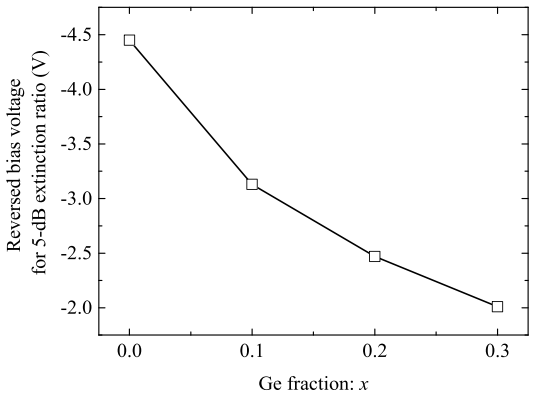

Fig. 16. Reversed bias voltage for 5-dB extinction ratio as a function of Ge fraction in SiGe alloy.

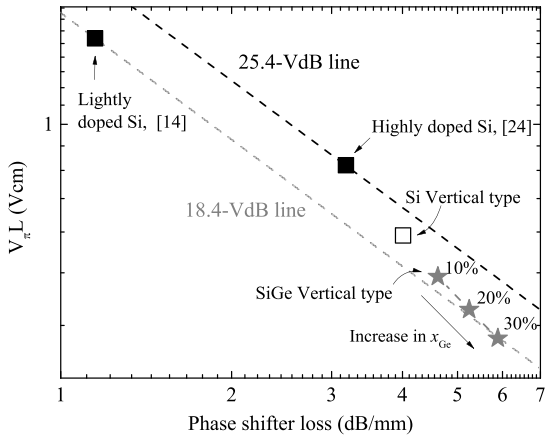

Fig. 17. $V_\pi L$ as a function of phase shifter loss of Si and SiGe modulators.

in strained SiGe. It is shown that the enhancement is still expected even considering the increased loss by strained SiGe, indicating strained SiGe is effective in terms of the modulation efficiency and the insertion loss.

In conjunction with the changes in the effective refractive index changes in Fig. 10, we calculate the transfer characteristics of symmetric SiGe MZI modulators by the transfer-matrix method as shown in Fig. 15. Modulation with an extinction ratio larger than -5 dB can be obtained in a symmetric $Si_{0.7}Ge_{0.3}$ MZI modulator with a 1-mm-long phase shifter when the reverse bias voltage is -2 V.

Figure 16 shows the reverse bias voltage required for a 5dB extinction ratio of the SiGe modulator as a function of the Ge fraction when the phase shifter length is 1000 μm. Using $Si_{0.7}Ge_{0.3}$, the driving voltage required for a 5dB extinction ratio can be reduced to less than half of that for a Si modulator. To discuss the device performance taking the loss of the phase shifter into account, $V_\pi L$ at -2 V as a function of the phase-shifter loss is shown in Fig. 17. In general, $V_\pi L$ can be reduced by increasing a hole density. However, the value of $\alpha V_\pi L$ increases since the increase in the phase-shifter loss is greater than the decrease in $V_\pi L$. Although the highly doped Si modulator in [26] can exhibit a low $V_\pi L$, the value of $\alpha V_\pi L$ is increased to approximately 25.4 V-dB higher than that for the lightly doped Si modulator in [14]. Because the Si modulator with a vertical *p-n* junction exhibits a high modulation efficiency; the value of $\alpha V_\pi L$ is under the 25.4 V-dB line in Fig. 17 for the Si modulator, it is worth noting that the value of $\alpha V_\pi L$ is even lower further owing to the enhanced plasma dispersion effect in strained SiGe. Thus, we can achieve a low $V_\pi L$ with maintaining $\alpha V_\pi L$ at a value comparable to that of a lightly doped Si modulator when the Ge fraction is 0.3.

In terms of modulation speed, SiGe is expected to be effective for faster RF response due to the short minority lifetime in SiGe in the case of the carrier-injection modulator [27]. However, it is not expected for the carrier-depletion modulator based on majority carriers. We expect that the crystal quality of SiGe is high enough for depletion modulators because the SiGe thickness considered in this paper is less than its critical thickness. Although the dielectric constant of the $Si_{0.7}Ge_{0.3}$ is slightly higher than Si, the increase in the depletion capacitance is negligible for the modulation speed. Thus, we expect that the introduction of SiGe has no negative impact of the modulation speed in terms of the material quality of SiGe. When the $V_\pi L$ of the SiGe modulator is designed to the same as the Si modulator, we can reduce the depletion capacitance of the SiGe modulator because of the enhanced plasma dispersion effect in SiGe. This means that the SiGe modulator can operate at higher modulation speed than Si modulators.

IV. Conclusion

We have numerically analyzed a carrier-depletion strained SiGe modulator with a vertical *p-n* junction. We have found that a vertical *p-n* junction shows approximately two times higher modulation efficiency than a lateral *p-n* junction, which is suitable for utilizing strained SiGe. By optimizing the doping concentration of the *p-n* junction, it was predicted that a strained $Si_{0.7}Ge_{0.3}$ optical modulator exhibits a modulation efficiency, $V_\pi L$ at 1.55 μm, of 0.31 V-cm at -2 V, which is approximately 1.8 times smaller than that of a Si optical modulator owing to the enhanced plasma dispersion effect in strained SiGe. Despite the high doping concentration of the *p-n* junction to obtain the low value of $V_\pi L$, the low $\alpha V_\pi L$ of 18.3 VdB, which is comparable to that for a lightly doped Si modulator, can be simultaneously obtained. Hence, the strained SiGe modulator based on carrier depletion can fundamentally improve the performance of Si-based optical modulators in terms of modulation efficiency and insertion loss.

References

[1] G. T. Reed, G. Mashanovich, F. Y. Gardes, and D. J. Thomson, "Silicon optical modulators," *Nature Photon.*, vol. 4, pp. 518–526, Jul. 2010.

[2] Q. Xu, B. Schmidt, S. Pradhan, and M. Lipson, "Micrometre-scale silicon electro-optic modulator," *Nature*, vol. 435, pp. 325–327, May 2005.

[3] L. Liao *et al.*, "40 Gbit/s silicon optical modulator for highspeed applications," *Electron. Lett.*, vol. 43, no. 22, Oct. 2007.

[4] A. Liu *et al.*, "High-speed optical modulation based on carrier depletion in a silicon waveguide," *Opt. Exp.*, vol. 15, no. 2, pp. 660–668, Jan. 2007.

[5] A. Liu *et al.*, "A high-speed silicon optical modulator based on a metal–oxide–semiconductor capacitor," *Nature*, vol. 427, pp. 615–618, Feb. 2004.

[6] F. Y. Gardes, D. J. Thomson, N. G. Emerson, and G. T. Reed, "40 Gb/s silicon photonics modulator for TE and TM polarisations," *Opt. Exp.*, vol. 19, no. 12, pp. 11804–11814, Jun. 2011.

[7] Y.-H. Kuo *et al.*, "Strong quantum-confined Stark effect in germanium quantum-well structures on silicon," *Nature*, vol. 437, pp. 1334–1336, Oct. 2005.

[8] J. Liu *et al.*, "Waveguide-integrated, ultralow-energy GeSi electro-absorption modulators," *Nature Photon.*, vol. 2, pp. 433–437, Jul. 2008.

[9] R. S. Jacobsen *et al.*, "Strained silicon as a new electro-optic material," *Nature*, vol. 441, pp. 199–202, May 2006.

[10] D. J. Thomson *et al.*, "50-Gb/s silicon optical modulator," *IEEE Photon. Technol. Lett.*, vol. 24, no. 4, pp. 234–236, Feb. 15, 2012.

[11] X. Tu *et al.*, "50-Gb/s silicon optical modulator with traveling-wave electrodes," *Opt. Exp.*, vol. 21, no. 10, pp. 12776–12782, May 2013.

[12] J. Ding, R. Ji, L. Zhang, and L. Yang, "Electro-optical response analysis of a 40 Gb/s silicon Mach–Zehnder optical modulator," *J. Lightw. Technol.*, vol. 31, no. 14, pp. 2434–2440, Jul. 15, 2013.

[13] T. Baehr-Jones *et al.*, "Ultralow drive voltage silicon traveling-wave modulator," *Opt. Exp.*, vol. 20, no. 11, pp. 12014–12020, May 2012.

[14] D. M. Gill *et al.* (2012). "A figure of merit based transmitter link penalty calculation for CMOS-compatible plasma-dispersion electro-optic Mach–Zehnder modulators." [Online]. Available: http://arxiv.org/abs/1211.2419

[15] I. Goykhman, B. Desiatov, S. Ben-Ezra, J. Shappir, and U. Levy, "Optimization of efficiency-loss figure of merit in carrier-depletion silicon Mach–Zehnder optical modulator," *Opt. Exp.*, vol. 21, no. 17, pp. 19518–19529, Aug. 2013.

[16] M. Takenaka and S. Takagi, "Strain engineering of plasma dispersion effect for SiGe optical modulators," *IEEE J. Quantum Electron.*, vol. 48, no. 1, pp. 8–16, Jan. 2012.

[17] Y. Kim, M. Takenaka, T. Osada, M. Hata, and S. Takagi, "Strain-induced enhancement of plasma dispersion effect and free-carrier absorption in SiGe optical modulators," *Sci. Rep.*, vol. 4, Apr. 2014, Art. ID 4683.

[18] R. People and J. C. Bean, "Calculation of critical layer thickness versus lattice mismatch for Ge_xSi_{1-x}/Si strained-layer heterostructures," *Appl. Phys. Lett.*, vol. 47, no. 3, pp. 322–324, 1985.

[19] R. People and J. C. Bean, "Erratum: Calculation of critical layer thickness versus lattice mismatch for Ge_xSi_{1-x}/Si strained-layer heterostructures," *Appl. Phys. Lett.*, vol. 49, no. 4, p. 229, 1986.

[20] P. Majhi *et al.*, "Demonstration of high-performance PMOSFETs using $Si-Si_xGe_{1-x}-Si$ quantum wells with high-κ/metal-gate stacks," *IEEE Electron Device Lett.*, vol. 29, no. 1, pp. 99–101, Jan. 2008.

[21] Y. Kim, M. Takenaka, T. Osada, M. Hata, and S. Takagi, "Fabrication and evaluation of propagation loss of Si/SiGe/Si photonic-wire waveguides for Si based optical modulator," *Thin Solid Films*, vol. 557, pp. 342–345, Apr. 2014.

[22] M. Miura, J. Fujikata, M. Noguchi, and Y. Arakawa, "Ultra-small butt-joint Ge photodetector featuring self-aligned *in-situ* doping and CMP-free novel CVD process," in *Proc. Opt. Fiber Commun. Conf. Exhibit.*, San Francisco, CA, USA, Mar. 2014, pp. 1–3.

[23] A. Liu *et al.*, "High-speed optical modulation based on carrier depletion in a silicon waveguide," *Opt. Exp.*, vol. 15, no. 2, pp. 660–668, 2007.

[24] R. A. Soref and B. R. Bennett, "Electrooptical effects in silicon," *IEEE J. Quantum Electron.*, vol. 23, no. 1, pp. 123–129, Jan. 1987.

[25] J. Van Campenhout, W. M. J. Green, and Y. A. Vlasov, "Design of a digital, ultra-broadband electro-optic switch for reconfigurable optical networks-on-chip," *Opt. Exp.*, vol. 17, no. 26, pp. 23793–23808, Dec. 2009.

[26] J. C. Rosenberg *et al.*, "A 25 Gbps silicon microring modulator based on an interleaved junction," *Opt. Exp.*, vol. 20, no. 24, pp. 26411–26423, Nov. 2012.

[27] Y. Kim, J. Fujikata, S. Takahashi, M. Takenaka, and S. Takagi, "Record-low injection-current strained SiGe variable optical attenuator with optimized lateral PIN junction," in *Proc. Eur. Conf. Opt. Commun.*, Cannes, France, Sep. 2014, pp. 1–3.

Younghyun Kim received the B.S. degree in electrical and electronic engineering from the University of Tokushima, Tokushima, Japan, and the M.S. degree from The University of Tokyo, Tokyo, Japan, in 2010 and 2012, respectively, where he is currently pursuing the Ph.D. degree.

Mr. Kim is a member of the Japan Society of Applied Physics.

Mitsuru Takenaka (M'02) was born in Kobe, Japan, in 1975. He received the B.E., M.E., and Ph.D. degrees in electronics engineering from The University of Tokyo, Japan, in 1998, 2000, and 2003, respectively.

He was a Research Fellow with the Optoelectronics Industry and Technology Development Association from 2003 to 2007, where he was involved in research on photonic routers. In 2007, he joined the Department of Electrical Engineering, The University of Tokyo, as a Lecturer. In 2008, he became an Associate Professor with the Department of Electrical Engineering and Information Systems, The University of Tokyo, where he currently works. His research interests presently focus on heterogeneous integration for III–V/Ge CMOS transistors and III–V/Si CMOS photonics.

Dr. Takenaka is a member of the IEEE Photonics Society, the IEEE Electron Devices Society, the Institute of Electronics, Information, and Communication Engineers (IEICE), and the Japan Society of Applied Physics (JSAP). He was a recipient of the Young Scientist Award for the Presentation of an Excellent Paper from JSAP in 2003, and the Young Researchers' Award from IEICE in 2005.

Shinichi Takagi (M'93) received the B.S., M.S., and Ph.D. degrees in electronics engineering from The University of Tokyo, in 1982, 1984, and 1987, respectively.

He is currently a Professor with the Department of Electrical Engineering and Information Systems, School of Engineering, The University of Tokyo.